In-situ Cure Monitoring of Epoxy/Graphene Nanocomposites by Several Spectroscopic Techniques

Vanesa Yuste-Sánchez[1]; Marianella Hernández Santana[1,*]; Tiberio A. Ezquerra[2]; Raquel Verdejo[1]; Miguel Angel López-Manchado[1]

[1] *Institute of Polymer Science and Technology (ICTP-CSIC), Juan de la Cierva 3, 28006 Madrid, Spain*

[2] *Institute for the Structure of the Matter (IEM-CSIC), Serrano 121, 28006, Madrid, Spain*

*corresponding author: marherna@ictp.csic.es

Abstract

Cure protocols of thermoset resins usually comprise two isothermal steps where resins undergo molecular cross-linking processes. The cure conditions are crucial to ensure a consistent and reliable manufacturing of the piece and have been the subject of an important body of research. While most studies have been carried out by traditional calorimetry or infrared spectroscopy under dynamic conditions, the development of new sensors and in-situ characterization techniques has resulted on a renewed interest on the subject under industrial isothermal protocols. Here, we monitor the curing reaction of both un-filled and nanofilled epoxy resin using broadband dielectric spectroscopy (BDS) and correlate the results with in-situ FT-IR and Raman spectroscopy. Hence, the proposed methodology provides complementary information on the chemical reactions and molecular dynamics associated to the cure cycle and can be an efficient tool for real-time monitorization of thermoset composites manufacturing.

Keywords: epoxy resin, graphene, nanocomposite, in-situ curing, broadband dielectric spectroscopy

1. INTRODUCTION

Curing of thermoset resin is accomplished in industry according to certain protocols suggested by resin manufacturers. Each resin has its own "industrial processing recipe" composed of strict temperature and time conditions aimed at achieving optimal properties and performances. Hence, it is mandatory for manufacturers and industries to comprehend the chemical reactions and the underlying physical changes occurring in the resin when following the suggested curing and post-curing conditions. Understanding these features and the whole cure cycle will provide quality control and avoid potential structural failures in parts due to under-curing and/or premature demolding.

A number of conventional techniques, such as differential scanning calorimetry (DSC), dynamic mechanical analysis (DMA), infrared spectroscopy (FT-IR) and Raman spectroscopy, have been used for cure monitoring and for predicting resin key properties [1-6]. Among them, broadband dielectric spectroscopy (BDS) also referred to as dielectric analysis (DEA) or as impedance spectroscopy, appears to be the most promising and popular method, although in many cases the reported measurements are non-isothermal and the preferred frequency range is not as adequate as expected [7]. BDS has been shown to be a powerful technique in order to follow in real time kinetics of relevant processes as crystallization [8, 9]. Moreover, several published studies [2, 3, 10-15] have demonstrated the usefulness of dielectric measurements for monitoring the curing reaction of thermosets. Senturia *et al*. [11] commented and reviewed various indirect methods that have been employed to analyze dielectric relaxations in curing systems. Zahouily *et al*. [3] investigated the kinetics of cationic and radical photopolymerization by using both real-time FT-IR spectroscopy and dielectric analysis. For a given UV curable formulation, a correlation was established between the extent of monomer conversion during the photopolymerization and the dielectric properties of the polymer obtained. Pethrick *et al*. [2] studied the changes in physical properties during and after the cure of a blend composed of an epoxy resin system with a poly(ether sulfone). They concluded that the use of real-time dielectric measurements during curing can be a very useful tool for the morphological characterization of phase-separated structures. They demonstrated that at high thermoplastic content (< 20 %) a distinct relaxation process dependent of the time of cure appears, ascribed to the

polarization of the occluded thermoplastic phase. While Müller *et al.* [15] determined the degree of curing of melamine-formaldehyde resins from the changes in ion viscosity. Their dielectric spectroscopy results were proven by correlating them with dynamic mechanical analysis and differential scanning calorimetry.

In a similar approach, monitoring the curing of epoxy composites has been also reported. Partially cured epoxy/organoclay nanocomposite samples were analyzed by Preda *et al*. [14] They investigated the influence of post thermal treatment on the dielectric response of the materials. After considering the samples as dielectrically stable, their properties were studied using BDS. They studied conduction and electrode polarization phenomena observed at low frequencies and the effect of water uptake on the dielectric behavior of the nanocomposite. On the other hand, Polansky *et al*. [7] developed a portable measuring system using impedance spectroscopy, for the on-line monitoring of epoxy/glass fiber composites curing and post-curing simulating industrial conditions. Their results were supported by other established methods for determining the degree of curing. While Jacobsen *et al*. [16] quantified the residual stress state building up during curing in a chopped strand mat (CSM) glass/epoxy composite and Kim *et al*. [17, 18] established correlations between dielectric properties and the key processing transitions of minimum viscosity, gelation and vitrification of carbon fiber/epoxy composite prepregs using impedance spectroscopy.

According to McIlhagger *et al.* [19] the application of dielectric measurements has been prevented by the limited availability of robust sensors and instrumentation suitable for the industrial environment. In line with this statement, most of the studies herein reported have developed alternative measuring configurations with tailored-made tool mounted sensors.

Despite all these previous investigations, establishing proper chemical kinetics and correct relations between state of cure, temperature, and the various dielectric magnitudes and relaxations is still a matter of research [20]. In addition, to the best of the authors´ knowledge, nothing has been reported considering both curing and post-curing stages of an epoxy/graphene nanocomposite. Thus, the aim of this research is to understand the underlying chemical processes that occur in an epoxy/graphene nanocomposite as it cures and post-cures and correlate them to the corresponding

changes in dielectric properties and molecular relaxations occurring in the network. In order to do so, a systematic *in-situ* measurement protocol was designed simulating industrial curing and post-curing settings. Contrary to what has been reported elsewhere [7], isothermal curing and post-curing cycles were considered employing a commercial broadband dielectric spectrometer, instead of tailored-made devices coupled to a hot press. The evolution of curing was also followed by FT-IR and Raman spectroscopy. The methodology herein discussed will serve as a reliable way for manufacturers and industries to control the curing process of a thermoset resin and to guarantee the trustworthiness of the suggested processing conditions and cure cycle.

2. EXPERIMENTAL

2.1. Materials

An epoxy resin based on diglycidyl ether of bisphenol A (DGEBA), commercially known as Araldite® XB 5940, and an anhydride type hardener Aradur® HY 5914 was supplied by *Hunstman* (see Figure 1). A resin:hardener 80:20 mix ratio in parts by weight was used according to the supplier specifications. Thermally reduced graphene oxide (TRGO) avING-1 was supplied by *Avanzare*.

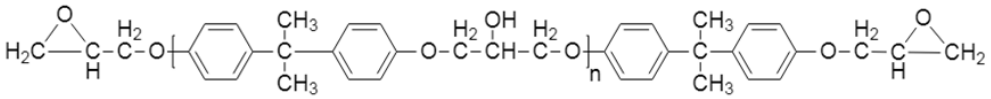

Figure 1. Diglycidyl ether of bisphenol A (DGEBA).

Epoxy/TRGO nanocomposites were prepared with 1 wt. % of filler. TRGO was initially dispersed in the resin using a three-roll mill (*Exakt 80 E*) following the conditions established in previous studies (Table 1) [21, 22]. Then, the nanofluid was mixed thoroughly with the hardener to ensure homogeneity in a vacuum reactor at 2400 rpm and 60 °C for 45 min.

Table 1. Mixing conditions of epoxy/TRGO nanofluids in a three roll mill.

	Gap 1 (μm)	Gap 2 (μm)	Speed (rpm)	Time (min)
Cycle 1	100	50	200	10
Cycle 2	50	25	250	10
Cycle 3	30	15	300	30

Samples (20 mm diameter and 1 mm thickness) were prepared by pouring a fixed amount of 375 ± 0.01 mg of the viscous resin or nanocomposite in a silicone mold preheated at 80 °C. A curing thermal treatment was applied placing the samples in an oven at 80 °C during 4 h, followed by a post-curing stage at 140 °C for 8 h.

2.2. *In-situ* Monitoring of the Curing and Post-Curing Reaction

2.2.1. Broadband Dielectric Spectroscopy Measuring Protocol

Broadband dielectric spectroscopy (BDS) measurements were performed on an ALPHA high resolution dielectric analyzer (*Novocontrol*). A supplementary characterization of oven cured and post-cured epoxy resin and epoxy/TRGO nanocomposite was followed. Samples were mounted in the dielectric cell between two parallel gold-plated electrodes. Consecutive isothermal frequency sweeps were measured over a frequency window of $10^{-1} < f/\text{Hz} < 10^{7}$ ($f = \omega/2\pi$ where f and ω are the frequency and angular frequency of the applied electric field) in the temperature range from room temperature to 150 °C in 5 °C steps with a ± 0.01 °C deviation in temperature. Resulting dielectric magnitudes are shown as Supporting Information S1.

In addition, a home-built dielectric cell assembly was designed for the *in-situ* monitoring of the isothermal curing and post-curing treatment of the epoxy resin and the epoxy/TRGO nanocomposite. As shown in Figure 2, the assembly consists of 4 elements: *i*) a tailor-made silicone ring with dimensions of 20 mm (internal diameter), 30 mm (external diameter), and 5 mm (depth); *ii*) a Kapton® spacer ring (0.1 mm, internal and external diameters 18 and 20 mm, respectively); *iii*) two gold plated electrodes (top and bottom electrodes) of 20 mm diameter and 2 mm thickness; *iv*) two gold plated electrodes (safety electrodes) of 30 and 40 mm diameter and 2 mm thickness. The bottom electrode was inserted inside the silicone ring, and the kapton

ring was placed on top of this electrode, to avoid any short circuit in case of contact between the lower and upper electrodes. Then, 375 ± 0.01 mg of un-cured resin were poured into the cavity and the top electrode was inserted closing the silicone ring cavity. A set of two extra bigger electrodes was included for safety reasons.

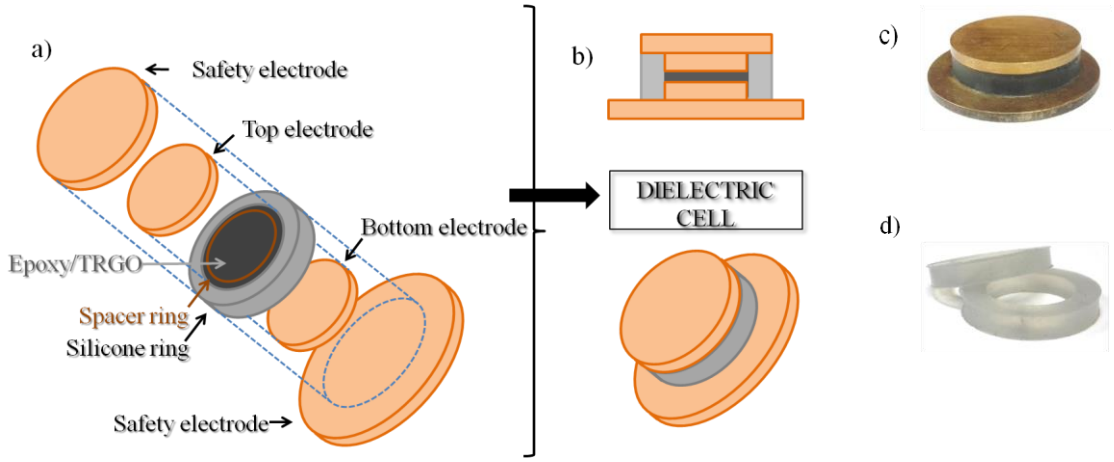

Figure 2. Dielectric cell: a) schematic assembly; b) cross-section; c) final setup; d) silicone ring.

A measuring protocol was designed to accurately simulate the in-situ isothermal curing and post-curing treatments of the epoxy resin and the epoxy/TRGO nanocomposite, as shown in Figure 3. The curing and post-curing conditions (temperature and time) were chosen according to a standard industrial protocol provided in the supplier´s data sheet. Room temperature samples were heated up to 80 °C and kept at that temperature during 4 h (curing stage). A second heating up to 140 °C was performed, maintaining that temperature during 8 h (post-curing stage). Then, samples were cooled down to room temperature. The average heating/cooling rate was of 2 °C/min. Dielectric magnitudes and their evolution with the thermal treatment were recorded every 30 min over a frequency window of $10^{-1} < f/\text{Hz} < 10^{7}$. At least, 3 measurements were done for each sample and the experimental error was 1 %.

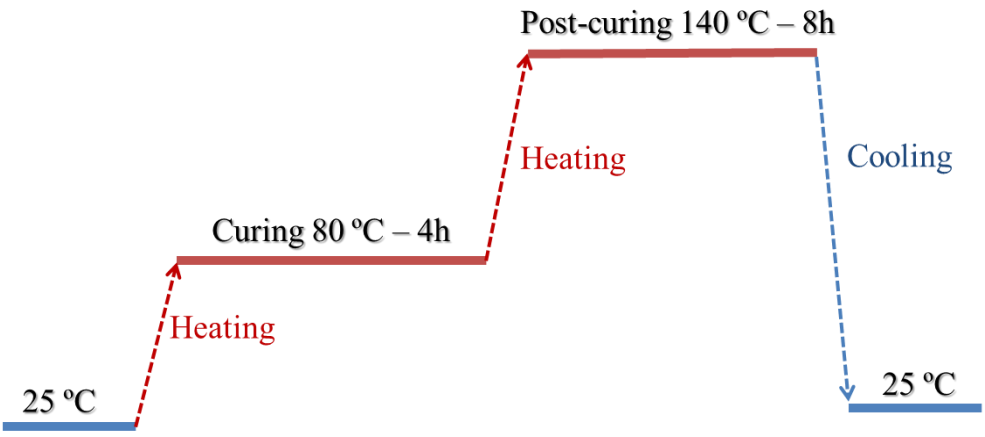

Figure 3. Thermal treatment protocol for monitoring in-situ curing and post-curing stages.

2.2.2. Fourier Transform Infrared Spectroscopy (FT-IR)

IR spectra were collected on a Spectrum One Spectrometer (*Perkin Elmer*) to gain insight into the structural changes occurring during the curing stage of the epoxy resin and the epoxy/TRGO nanocomposite as a function of time. Data were collected from 4000 cm^{-1} to 700 cm^{-1} at a resolution of 4 cm^{-1}. A curing cell consisting of two circular KBr crystals embedded in a metallic heating frame was coupled to the spectrometer (see Supporting Information S2). One drop of either the fluid resin or of the nanocomposite was added between the two crystals in order to monitor the evolution of the curing process with time. Once the curing temperature (80 °C) was reached, data were collected every minute during 4 h. A reference spectrum was collected from cleaned KBr crystals at a resolution of 4 cm^{-1}. At least, 3 measurements were done for each sample.

The reaction kinetics was determined from the comparison of the spectra at different intervals, based on the evolution of specific absorbance bands, referred to as "*x*" in equation 1, corresponding to the functional groups appearing and/or disappearing during the curing reaction. The extent of reaction or conversion degree was calculated by taking as reference an invariant band located at 1510 cm^{-1}, corresponding to the C-C bonds of the aromatic ring according to the following ratio [23, 24]:

$$\alpha_{IR}\ (t) = 1 - \left[\frac{I_x(t)/I_{1510}(t)}{I_x(0)/I_{1510}(0)}\right] \quad \text{(eq. 1)}$$

where $I(t)$ and $I(0)$ correspond to the peak area at time "*t*" and at the beginning of curing (*t*=0), and "ref" corresponds to the reference peak, respectively.

2.2.3. Raman Spectroscopy

Raman spectroscopy was performed using a Raman spectrometer (*Renishaw 2000*) with an acquisition time of 15 min during 4 h at 80 °C to monitor the curing reaction. The spectral region from 1500 to 1950 cm^{-1} was collected using a laser with an excitation line of wavelength λ=514 nm. At least, 3 measurements were done for each sample.

In order to determine the degree of conversion of each functional group during the curing reaction, the intensity of specific spectral bands, referred to as "*x*" in equation 2, was normalized by a reference band located at 1609 cm^{-1}, as follows:

$$\alpha_{RAMAN}(t) = 1 - \left[\frac{I_x(t)/I_{1609}(t)}{I_x(0)/I_{1609}(0)}\right] \quad \text{(eq. 2)}$$

where $I(t)$ and $I(0)$correspond to the peak intensity at time "*t*" and at the beginning of curing (*t*=0), and "ref" corresponds to the reference peak, respectively.

3. RESULTS AND DISCUSSION

Although the curing process of an epoxy resin is well understood, the one of an epoxy nanocomposite is not. In general, during curing, an epoxy resin goes through several stages. In the first stage, the resin changes from a liquid state with minimum viscosity to a gelation state. Then, as curing proceeds, the resin reaches vitrification converting the gel into a vitreous crosslinked solid. At a second stage, normally known as post-curing, the resin undergoes further heating to achieve full cure, the chemical network is hardened and the expected mechanical rigidity is obtained.

In the following sections, a systematic *in-situ* study of the dielectric behavior of an epoxy resin and an epoxy/TRGO nanocomposite is presented. Results are discussed based on the changes of the dielectric magnitudes according to the stages of the curing process.

3.1. Stage I: Curing

3.1.1. Evolution of Dielectric Properties of Epoxy Resin and Epoxy/TRGO Nanocomposite during Curing

Samples subjected to the isothermal *in-situ* curing protocol previously described (Figure 3) were analyzed aiming to understand the relation between the chemical kinetics of a thermosetting system and the corresponding changes in dielectric properties. From the dielectric point of view, a curing process is dominated by two different mechanisms: 1) the migration of ion or charged molecules highly influenced by the viscosity of the system, and 2) the dipolar response related to the motions of the chains that begin to crosslink [3, 13, 25, 26]. Thus, two dielectric magnitudes are of special interest. Firstly, the ionic conductivity that appears as a key magnitude at early stages of curing. According to several authors [3, 11, 13, 17], the electrical conductivity, the real part of the complex electrical conductivity, is perhaps the most useful overall probe of cure state, since for most polymers, electrical conductivity follows closely the changes in viscosity. Secondly, the dielectric loss, imaginary part of the dielectric permittivity, can be very useful to monitor relaxation processes occurring at molecular level taking place during the vitrification of the resin system. Figure 4 shows the evolution with curing time of these two dielectric magnitudes as a function of frequency for an epoxy resin and for an epoxy/TRGO nanocomposite.

At the initial stages of the curing process, the conductivity curves of the resin show three well differentiated regions characteristic of ionic liquids [27, 28], as seen in Figure 4a. In the low frequencies region, an increment on conductivity associated to blocking effects in the electrodes is observed; during the mid-frequencies, a plateau associated to the DC conductivity is observed; while at high frequencies, an AC contribution associated to dispersion sets in. As the curing process continues, the three distinguished

regions tend to convert into a well-defined plateau at low frequency and a frequency dependent conductivity region at higher frequencies. During curing it is expected that viscosity increases and limits the motion of ion or charged molecules, that is, the ionic contribution is hindered by the gelation of the matrix [12, 13, 29]. Several authors attribute this ionic contribution to the translational movement of Na^+ and Cl^- ions left from the synthesis of epoxy systems [3, 12, 13, 26, 29].

Additionally, in the initial stage, conductivity data exhibit a bump at higher frequencies that shifts towards lower frequencies as curing time proceeds. In order to evaluate the origin of this contribution, the dielectric loss has been represented in Figure 4c. By doing this, the conductivity appears as a frequency dependent contribution that decreases linearly, while relaxation processes appear as maxima. The molecular dipolar relaxation response becomes detectable in the initial stage as a maximum in the permittivity loss in the same frequency range as the corresponding bump observed in the conductivity measurements. This maximum shifts to lower frequencies when increasing curing time and it can be ascribed to the segmental relaxation.

For comparison purposes, the segmental relaxation of an oven-cured resin is presented as Supporting Information, S1. The evolution of this relaxation with curing time can be interpreted as consequence of the polymer chain restrictions during the curing process, and thus, be associated to the vitrification of the matrix where cooperative motion cannot occur due to the insufficient free volume [17]. A curing time of 3 h seems to be a critical point in the curing process, after which the segmental relaxation is no longer noticeable, and thus vitrification seems to be completed.

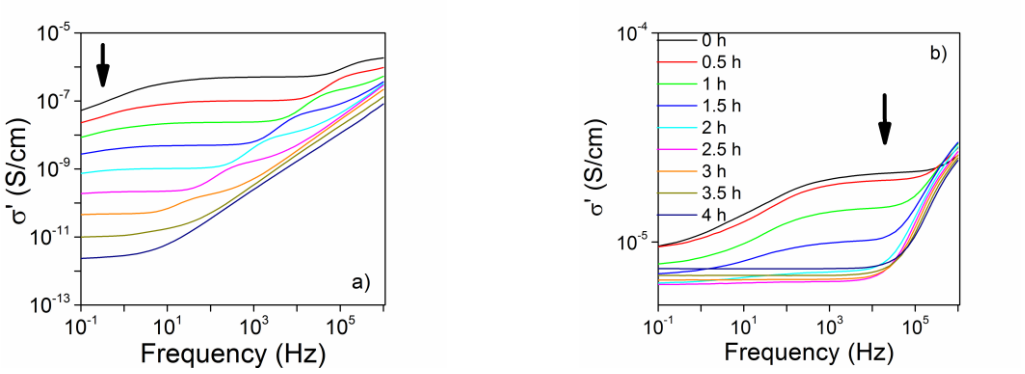

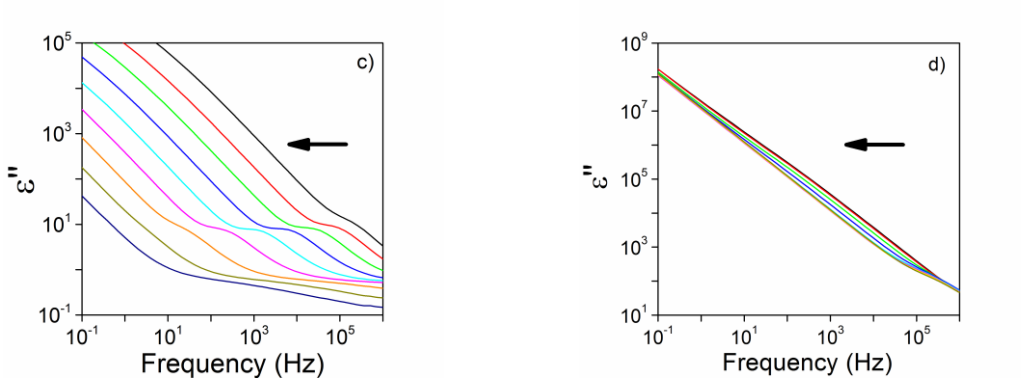

Figure 4. Evolution of dielectric magnitudes (conductivity and permittivity loss) with curing time and frequency of: a), c) epoxy resin; b), d) epoxy/TRGO nanocomposite. Arrows indicate evolution with curing time (30 min intervals).

For a deeper understanding of the dielectric behavior, data extracted from selected frequencies from Figure 4 are plotted in Figure 5. At 3 h, it looks that curing rate starts to reach maximum values, and a rapid change on conductivity with time is observed (see Figure 5a). Towards the end of cure, conductivity seems to level out, especially at high frequencies. Similar results were found by Zahouily *et al*. [3] They followed the evolution of electrical resistivity with irradiation time of a UV-cured epoxy resin and found that as curing reaction proceeds, a decrease in ion mobility due to crosslinking occurs. As the reaction slows down, the rate of increase in ion viscosity also slows down; showing that cure is near completion. Since electrical conductivity and permittivity loss are related to each other, it is expected that both magnitudes reflect the same behavior in a different manner. A decrease in permittivity loss with time is noticed since ion and dipole mobility become more restricted as curing proceeds [1]. The point at which dipolar relaxation ceases to be detected corresponds to the vitrification of the matrix. Certain discrepancies are reported in the literature regarding the frequency at which vitrification can be detected. Pethrick *et al*. [2] used 10 kHz, while Kim *et al*. [17] use 0.1 Hz. Moreover, Day *et al.* [30] suggested that monitoring curing times at frequencies < 10 Hz, and > 10^3 Hz is inaccurate because blocking and polarization effects, and low sensitivity, respectively. Our study shows that conductivity and dielectric permittivity start to level off with curing time, as an indication of vitrification, from 10^2 Hz onwards, as seen in Figure 11.

The behavior of epoxy/TRGO nanocomposites differs from that of the pure resin. Adding conducting fillers like TRGO determines a change on the behavior of the dielectric magnitudes during curing, as shown in Figure 4b. The bump observed in the mid-frequencies on the conductivity curves shifts to lower frequencies as curing evolves, reaching a conducting plateau due to the inclusion of TRGO after 2 h of curing (Figure 5b). Hence, TRGO appears to accelerate the curing process of the epoxy resin. Furthermore, since the overall conductivity values of the epoxy/TRGO nanocomposite are between 1-8 orders of magnitude higher than those of the neat epoxy resin, the electrical conductivity contribution from the TRGO seems to mask the contributions occurring in the epoxy matrix [31, 32]. In fact, the permittivity loss data shown in Figure 4d only exhibit the conductivity contribution, characterized by a contribution that decreases linearly with the frequency on a Log-Log scale.

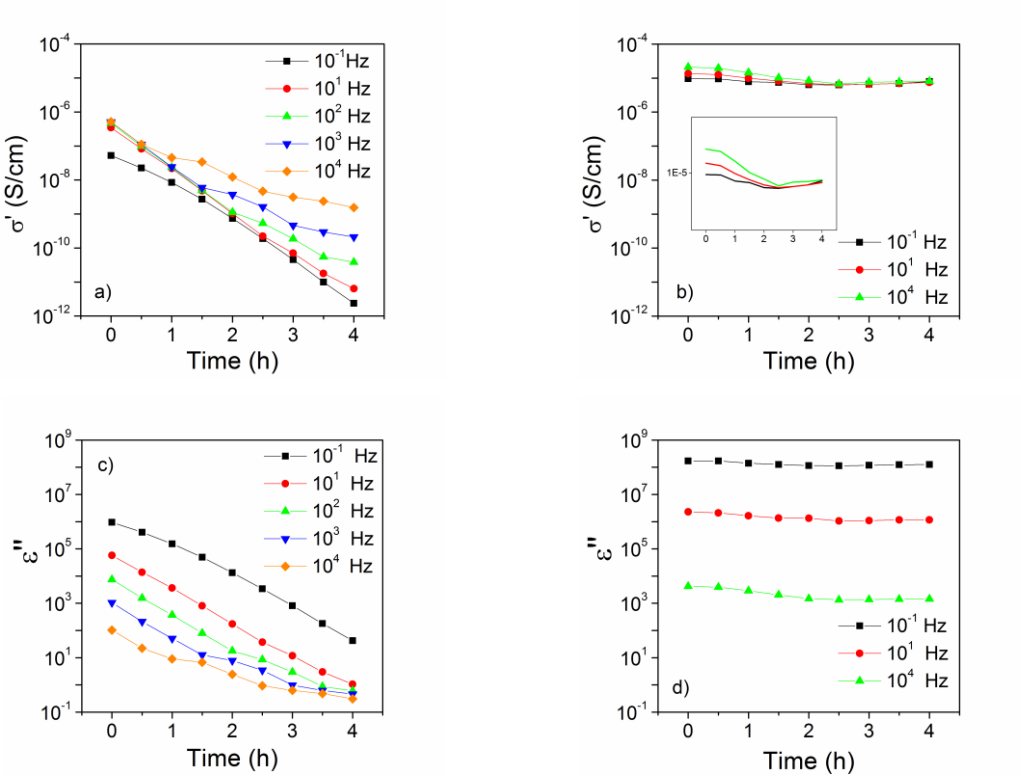

Figure 5. Evolution of the dielectric magnitudes (conductivity and permittivity loss) with curing time at selected frequencies: a), c) epoxy resin; and b), d) epoxy/TRGO nanocomposite.

3.1.2. Chemical Reactions Occurring During Curing of Epoxy Resin and Epoxy/TRGO Nanocomposite

The underlying chemical reactions occurring during the curing of a thermoset system composed of an epoxy resin and an anhydride-type hardener have been reported elsewhere [33, 34]. Three major reactions take place: *i*) secondary alcohols from the epoxy backbone react with the anhydride forming a mono-ester; *ii*) carboxylic acid reacts with an epoxy group forming a di-ester and a new secondary hydroxyl group; *iii*) epoxy groups react with a secondary alcohol forming a (*β*-hydroxy) ether linkage. The first two reactions are dominant reactions occurring in anhydride cured epoxy resin systems, with etherification occurring to a much lesser extent and at later stages. One can determine the extent of the curing reaction by following the appearance and/or disappearance of specific FT-IR spectral bands. As shown in Figure 6 the intensity of the bands located at 1860 and 1780 cm^{-1} ascribed to the stretching of C=O bonds of the anhydride hardener decrease with curing time [6], while the band located at 1740 cm^{-1}, corresponding to the formation of ester groups, increases [34, 35]. Both trends are a clear evidence of the curing reaction taking place in the epoxy resin as well as in the epoxy/TRGO nanocomposite. Spectral bands located at lower wavenumbers and associated to the etherification reaction [34, 36] are shown as Supporting Information S3.

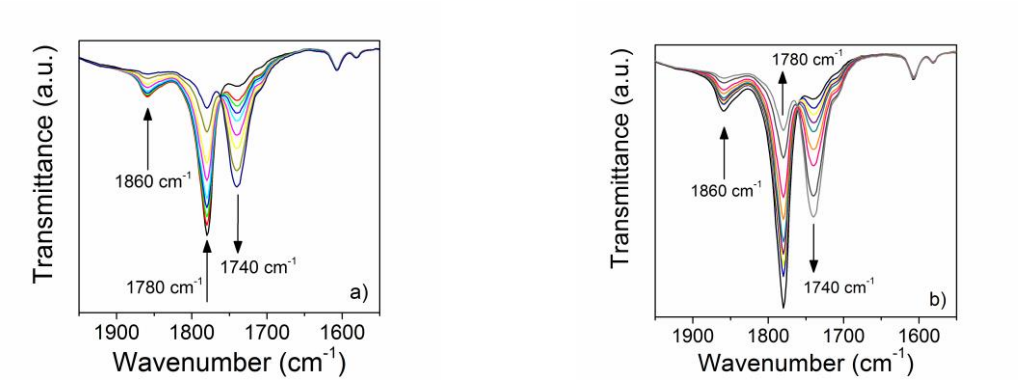

Figure 6. FT-IR spectra evolution with curing time of: a) epoxy resin; b) epoxy/TRGO nanocomposite. Arrows indicate evolution with curing time.

Raman spectroscopy also serves for monitoring the curing reaction of epoxy resins. The different spectra obtained at 80 °C during the curing step can be seen in Figure 7, showing the same trend with regard to the characteristic spectral bands: increase of the band at 1740 cm^{-1} (formation of ester groups), and decrease of the bands at 1780 and 1860 cm^{-1} (consumption of hardener). Unfortunately, following this type of reaction in an epoxy/TRGO nanocomposite was not possible due to the high conductivity of TRGO which hindered the identification of the corresponding spectral bands.

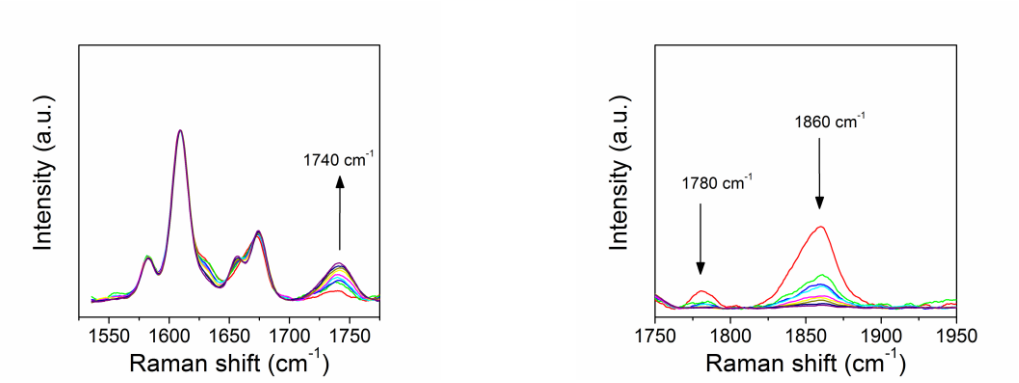

Figure 7. Raman spectra evolution with curing time of epoxy resin at different wavenumber ranges. Arrows indicates evolution with curing time.

3.1.3. Correlating Curing Kinetics with Dielectric Behavior of Epoxy Resin and Epoxy/TRGO Nanocomposite

The curing time dependent permittivity loss and conductivity results (see Figure 5) allow us to propose the following relations to monitor in real time their variation during the curing stage [1]:

$$\alpha_{\varepsilon}(t) = \frac{\log(\varepsilon''(0)) - log(\varepsilon''(t))}{log\,(\varepsilon''(0)) - log(\varepsilon''(t_{max}))} \qquad \text{(eq. 3)}$$

$$\alpha_{\sigma}(t) = \frac{\log(\sigma(0)) - \log(\sigma(t))}{\log(\sigma(0)) - \log(\sigma(t_{max}))} \qquad \text{(eq. 4)}$$

Where $\varepsilon''(0)$ is the permittivity loss at the beginning of curing, $\varepsilon''(t)$ is the permittivity loss at curing time "*t*", and $\varepsilon''(t_{max})$ is the permittivity loss at the end of the cure process, *i.e.* maximum time (4 h). Analogously, $\sigma(0)$ is the conductivity at the

beginning of curing, $\sigma(t)$ is the conductivity at curing time "t", and $\sigma(t_{max})$ is the conductivity at the end of the cure process, *i.e.* maximum time (4 h). Both magnitudes were recorded at $f = 10^4$ Hz.

Figure 8 shows the degree of conversion of the epoxy resin and the epoxy/TRGO nanocomposite based on the evolution of permittivity loss and conductivity. As expected, the trend for both magnitudes is similar. At the beginning, curing goes faster for the epoxy resin, reaching 50 % of conversion during the early stages of the curing process. Afterwards, crosslinking is accelerated by the presence of TRGO, accomplishing 100 % of curing after 2 h. The reaction of the epoxy resin on the other hand, progresses gradually up to 4 h.

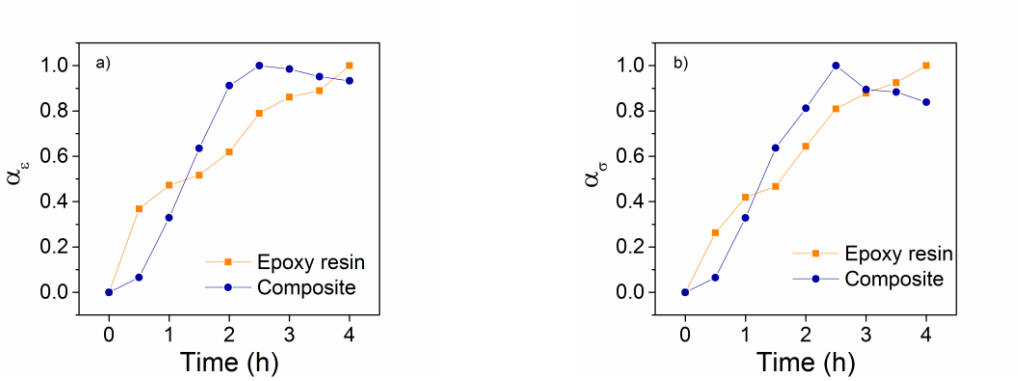

Figure 8. Degree of conversion of an epoxy resin and an epoxy/TRGO nanocomposite during curing based on: a) permittivity loss; and b) conductivity. Both magnitudes were recorded at $f = 10^4$ Hz.

Similarly, by FT-IR and Raman spectroscopy one can follow the conversion degree by discussing the changes on the bands at 1860 cm^{-1} (disappearance of hardener) and 1740 cm^{-1} (formation of ester groups), as shown in Figure 9. However, the quantitative analysis of the 1740 cm^{-1} band and its correlation with chemical species (ester groups) is not as straightforward since hydrogen bonding can occur inter- and intra-molecularly in the resin during curing, altering the quantification [4, 5]. Both techniques seem to support the same behavior. The epoxy resin tends to have a fast initial curing and then slows down after 2-3 h of reaction, while in presence of TRGO the curing reaction is accelerated.

Due to the fact that the three techniques (FT-IR, Raman spectroscopy, and dielectric spectroscopy) observe and measure different molecular probes, the conversion degrees from FT-IR and Raman do not exactly match those obtained by dielectric conversion. However, they all seem to coincide in the fact that a curing time of 3 h for the epoxy and of 2 h for the epoxy/TRGO nanocomposite appear as critical points. Shorter times will only lead to gelation of the resin, while going beyond that critical point will guarantee that optimal curing will be achieved. Moreover, establishing a good correlation between the three techniques allows us to understand simultaneously the chemical reactions and physical changes associated to gelation occurring during the cure cycle.

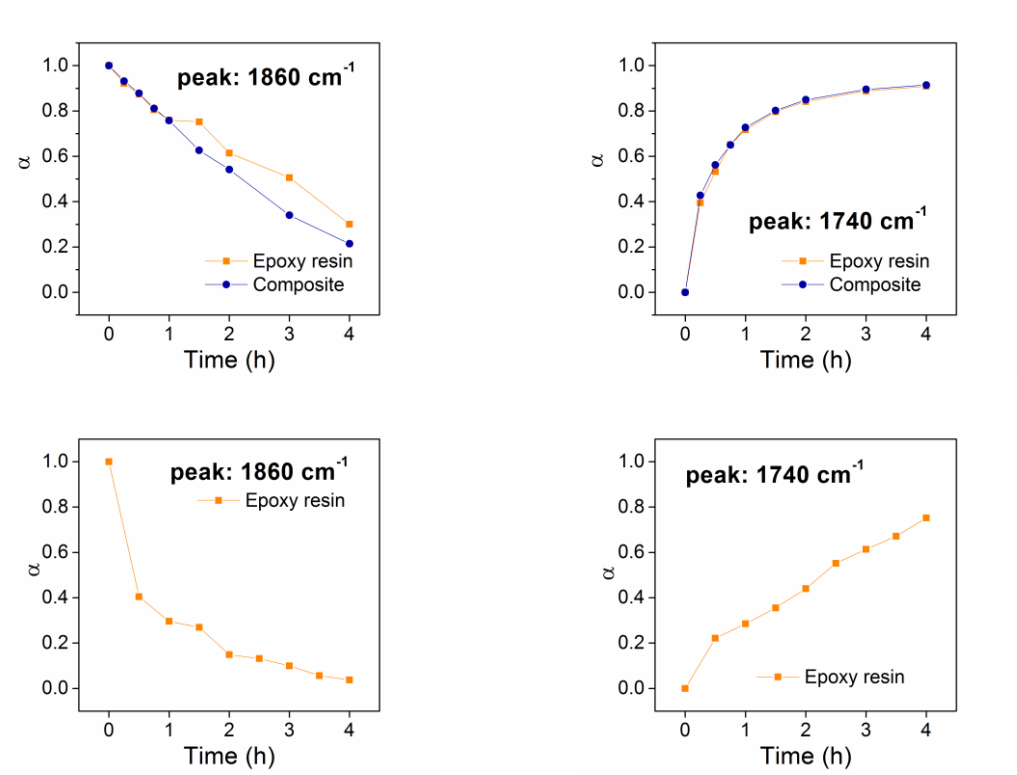

Figure 9. Conversion degree of epoxy resin and epoxy/graphene nanocomposite calculated from the changes in the area of selected peaks. Top: by FT-IR; bottom: by Raman spectroscopy.

3.2. Stage II: Post-Curing

As a rule of thumb, a post-curing stage is generally imposed for increasing the glass transition temperature and for improving the mechanical properties of the epoxy system. With regard to the dielectric behavior, a slight decrease in the conductivity of the resin and a shift of the permittivity loss to lower frequencies occur during post-curing, as seen in Figure 10. On the contrary, the variations on the epoxy/TRGO nanocomposite are inexistent. These variations are less significant than those obtained in the curing stage. During post-curing the noteworthy reduction in segmental mobility leads to a marked decrease in the rate of reaction, as the reaction becomes diffusion or mobility controlled. Consequently, the changes in the dielectric magnitudes with time and frequency are not as notorious as in the curing stage, as can be seen in Figure 11 [7, 11].

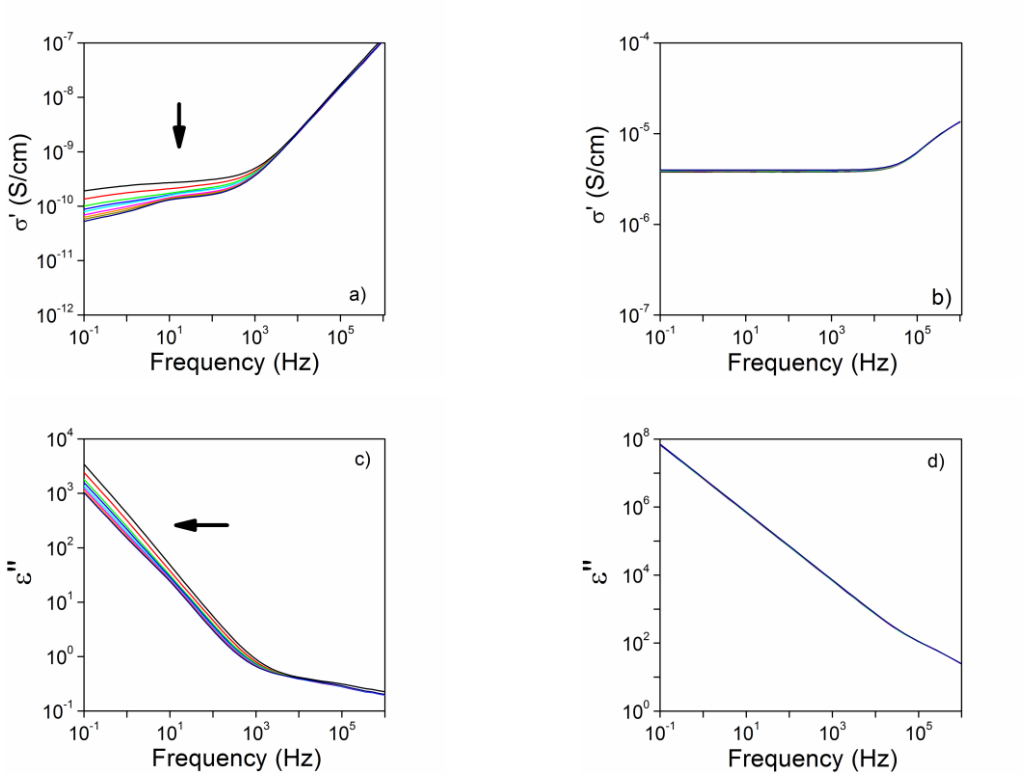

Figure 10. Evolution of dielectric magnitudes (conductivity and permittivity loss) during post-curing of: a), c) epoxy resin; b), d) epoxy/TRGO nanocomposite. Arrows indicate evolution with post-curing time (30 min intervals).

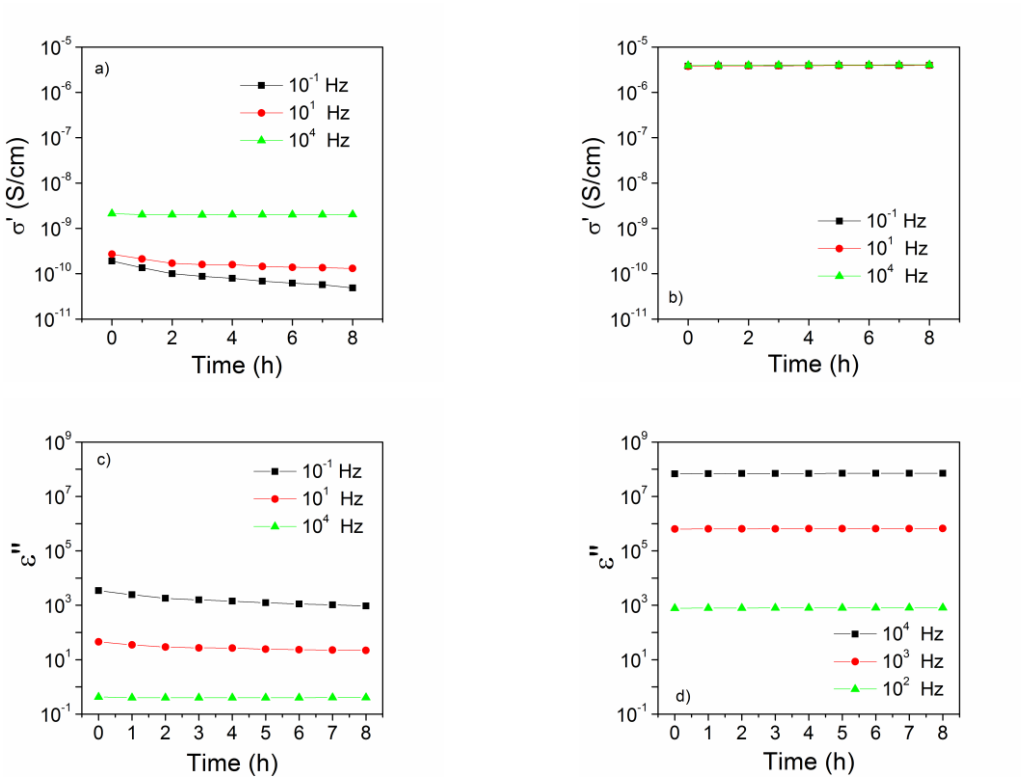

Figure 11. Evolution of dielectric magnitudes (conductivity and permittivity loss) with post-curing time at selected frequencies: a), c) epoxy resin; and b), d) epoxy/TRGO nanocomposite.

The complete cycle (curing + post-curing) of both the epoxy resin and epoxy/TRGO nanocomposite can be interpreted based on the evolution of an experimental measured magnitude, such as electrical conductivity, and its correlation with the materials properties (viscosity and degree of curing) as shown in Figure 12. With regard to the resin, during the heating ramp, conductivity reaches the maximum value due to the minimum viscosity and thereof highest ionic mobility. Once curing temperature is reached, conductivity decreases progressively due to mobility restrictions, as curing effects dominate over thermal effects. During the second heating ramp, the system is in a rubbery state and the molecules regain their mobility, allowing the diffusion-driven curing to slowly continue during the post-curing stage. This increase in mobility also favors motion of migrating charges, resulting in an increase of conductivity in the epoxy resin. Curing restricting effects dominate again over thermal effects and as post-curing proceeds conductivity tends to decrease but in a less notorious way. Finally, when cooling down conductivity drops considerably reaching typical values of isolating

dielectric materials at room temperature. The difference between initial and final conductivity can be ascribed to the differences in viscosity and thus in ionic mobility between a viscous fluid and a totally cured resin.

The changes are less notorious for the nanocomposite due to the electrical conductivity contribution from the TRGO that seems to mask both the dielectric relaxation and also the conductivity contribution of the epoxy matrix. Important to mention that initial and final conductivity values after completing the whole cure cycle are very similar. This is a promising result from a manufacturer´s point of view, since they can somehow predict final electrical properties based on the initial values of the nanocomposite before even curing.

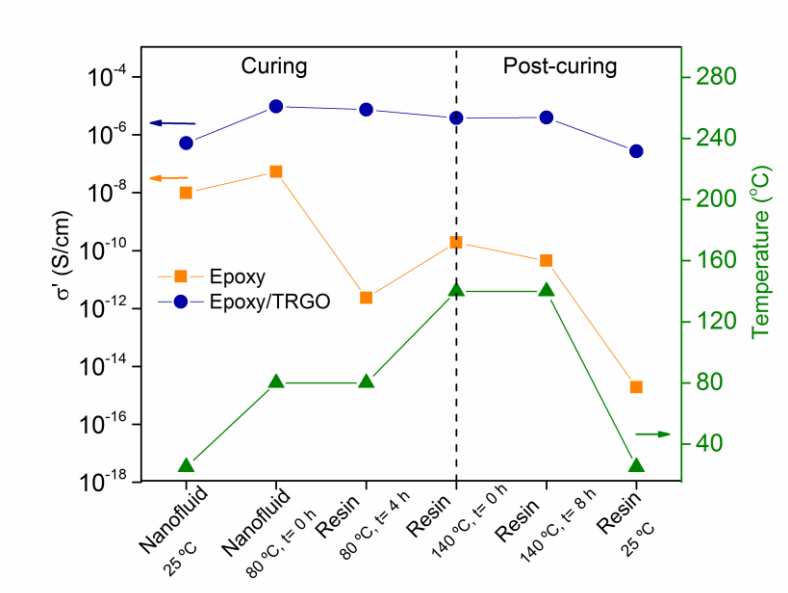

Figure 12. Conductivity evolution with the cure cycle (curing + post-curing) of an epoxy resin and epoxy/TRGO nanocomposite.

4. CONCLUSIONS

A measuring protocol for monitoring in real-time and *in-situ* the complete isothermal cure cycle (curing + post-curing) of an epoxy resin and an epoxy/TRGO nanocomposite has been designed using broadband dielectric spectroscopy. Results based on the evolution of two dielectric magnitudes (conductivity and permittivity loss) allow us to

conclude that curing of the resin occurs rapidly at the early stages and then progresses gradually. In presence of TRGO, crosslinking goes faster accomplishing 100 % of curing after 2 h. Chemical changes occurring during the thermal treatment were also studied by FT-IR and Raman spectroscopy in order to understand the underlying molecular changes taking place in the network. A curing time of 3 h for the epoxy resin and of 2 h for the epoxy/TRGO nanocomposite appear as critical times below which the formation of the crosslinked network will not occur. The changes occurring during the post-curing stage on the other hand, are less notorious and seem to haves less influence on the final properties of the resin and nanocomposite. This unique measuring protocol will serve as an efficient tool for the optimization of cure cycles of thermoset systems and thermoset composites.

ACKNOWLEDGEMENTS

The authors acknowledge the Ministry of Science, Innovation and Universities for research contracts (MAT2016-81138-R and RYC-2017-22837).

REFERENCES

[1] R. Hardis, J.L.P. Jessop, F.E. Peters, M.R. Kessler, Cure kinetics characterization and monitoring of an epoxy resin using DSC, Raman spectroscopy, and DEA, Composites Part A: Applied Science and Manufacturing, 49 (2013) 100-108.
[2] A.J. MacKinnon, S.D. Jenkins, P.T. McGrail, R.A. Pethrick, A dielectric, mechanical, rheological and electron microscopy study of cure and properties of a thermoplastic-modified epoxy resin, Macromolecules, 25 (1992) 3492-3499.
[3] K. Zahouily, C. Decker, E. Kaiserberger, M. Gruener, Cure Monitoring of UV-Curable Free Radical And Cationic Systems by Using In-situ Dielectric Analysis and Real-Time FT-Infrared Spectroscopy, RadTech UV & EB Technology Expo & ConferenceCharlotte, NC, 2004.
[4] S.-J. Park, G.-H. Kwak, M. Sumita, J.-R. Lee, Cure and reaction kinetics of an anhydride-cured epoxy resin catalyzed by N-benzylpyrazinium salts using near-infrared spectroscopy, Polymer Engineering & Science, 40 (2000) 2569-2576.
[5] G.A. George, P. Cole-Clarke, N. St. John, G. Friend, Real-time monitoring of the cure reaction of a TGDDM/DDS epoxy resin using fiber optic FT-IR, Journal of applied polymer science, 42 (1991) 643-657.
[6] J. Rocks, L. Rintoul, F. Vohwinkel, G. George, The kinetics and mechanism of cure of an amino-glycidyl epoxy resin by a co-anhydride as studied by FT-Raman spectroscopy, Polymer, 45 (2004) 6799-6811.

[7] R. Polanský, J. Pihera, J. Komárek, R. Pavlica, P. Prosr, J. Freisleben, R. Vik, K. Hromadka, T. Blecha, J. Čengery, R. Soukup, M. Čermák, M. Zemanová, P. Kadlec, A. Hamáček, Development of a measuring system for on-line in situ monitoring of composite materials manufacturing, Composites Part A: Applied Science and Manufacturing, 90 (2016) 760-770.
[8] A. Sanz, A. Nogales, T.A. Ezquerra, N. Lotti, A. Munari, S.S. Funari, Order and segmental mobility during polymer crystallization: Poly (butylene isophthalate), Polymer, 47 (2006) 1281-1290.
[9] A. Sanz, A. Nogales, T.A. Ezquerra, M. Soccio, A. Munari, N. Lotti, Cold Crystallization of Poly(trimethylene terephthalate) As Revealed by Simultaneous WAXS, SAXS, and Dielectric Spectroscopy, Macromolecules, 43 (2010) 671-679.
[10] D. Kranbuehl, S. Delos, E. Yi, J. Mayer, T. Jarvie, W. Winfree, T. Hou, Dynamic dielectric analysis: Nondestructive material evaluation and cure cycle monitoring, Polymer Engineering & Science, 26 (1986) 338-345.
[11] S.D. Senturia, N.F. Sheppard, Dielectric analysis of thermoset cure, Springer Berlin Heidelberg, Berlin, Heidelberg, 1986, pp. 1-47.
[12] C.Y. Shigue, R.G. dos Santos, C.A. Baldan, E. Ruppert-Filho, Monitoring the epoxy curing by the dielectric thermal analysis method, IEEE transactions on applied superconductivity, 14 (2004) 1173-1176.
[13] L. Garden, D. Hayward, R. Pethrick, Dielectric non-destructive testing approach to cure monitoring of adhesives and composites, Proceedings of the Institution of Mechanical Engineers, Part G: Journal of Aerospace Engineering, 221 (2007) 521-533.
[14] I. Preda, J. Castellon, S. Agnel, H. Couderc, M. Frechette, F. Gao, R. Nigmatullin, S. Thompson, A. Vaessen, Dielectric response of various partially cured epoxy nanocomposites, IEEE Transactions on Dielectrics and Electrical Insulation, 20 (2013) 580-591.
[15] U. Müller, C. Pretschuh, E. Zikulnig-Rusch, E. Dolezel-Horwath, M. Reiner, S. Knappe, Dielectric analysis as cure monitoring system for melamine-formaldehyde laminates, Progress in Organic Coatings, 90 (2016) 277-283.
[16] J. Jakobsen, A. Skordos, S. James, R.G. Correia, M. Jensen, In-situ Curing Strain Monitoring of a Flat Plate Residual Stress Specimen Using a Chopped Stand Mat Glass/Epoxy Composite as Test Material, Applied Composite Materials, 22 (2015) 805-822.
[17] D. Kim, T. Centea, S.R. Nutt, In-situ cure monitoring of an out-of-autoclave prepreg: Effects of out-time on viscosity, gelation and vitrification, Composites Science and Technology, 102 (2014) 132-138.
[18] D. Kim, T. Centea, S.R. Nutt, Out-time effects on cure kinetics and viscosity for an out-of-autoclave (OOA) prepreg: Modelling and monitoring, Composites Science and Technology, 100 (2014) 63-69.
[19] A. McIlhagger, D. Brown, B. Hill, The development of a dielectric system for the on-line cure monitoring of the resin transfer moulding process, Composites Part A: Applied Science and Manufacturing, 31 (2000) 1373-1381.
[20] M. Wlodarska, Curing Reaction and Dielectric Properties of Rigid and Elastic Liquid Crystal Epoxy Networks Modified with Nanofillers, International Journal of Polymer Science, (2018) 10.
[21] J.M. Vazquez-Moreno, V. Yuste-Sanchez, R. Sanchez-Hidalgo, R. Verdejo, M.A. Lopez-Manchado, L. Fernández-García, C. Blanco, R. Menéndez, Customizing thermally-reduced graphene oxides for electrically conductive or mechanical reinforced epoxy nanocomposites, European Polymer Journal, 93 (2017) 1-7.

[22] R. Sánchez-Hidalgo, V. Yuste-Sanchez, R. Verdejo, C. Blanco, M.A. Lopez-Manchado, R. Menéndez, Main structural features of graphene materials controlling the transport properties of epoxy resin-based composites, European Polymer Journal, 101 (2018) 56-65.
[23] R.E. Smith, F.N. Larsen, C.L. Long, Epoxy resin cure. II. FTIR analysis, Journal of Applied Polymer Science, 29 (1984) 3713-3726.
[24] F. Fraga, E.C. Vazquez, E. Rodríguez-Núñez, J.M. Martínez-Ageitos, Curing kinetics of the epoxy system diglycidyl ether of bisphenol A/isophoronediamine by Fourier transform infrared spectroscopy, Polymers for Advanced Technologies, 19 (2008) 1623-1628.
[25] G. Boiteux, P. Dublineau, M. Feve, C. Mathieu, G. Seytre, J. Ulanski, Dielectric and viscoelastic studies of curing epoxy-amine model systems, Polymer Bulletin, 30 (1993) 441-447.
[26] K.A. Nass, J.C. Seferis, Analysis of the dielectric response of thermosets during isothermal and nonisothermal cure, Polymer Engineering & Science, 29 (1989) 315-324.
[27] F. Kremer, Dynamics in geometrical confinement, Springer2014.
[28] A. Linares, M.J. Cánovas, T.A. Ezquerra, Nearly constant dielectric loss behavior in ionomers, The Journal of Chemical Physics, 128 (2008) 244908.
[29] F. Stephan, G. Seytre, G. Boiteux, J. Ulanski, Study of dielectric response of PMR-15 resin during cure, Journal of Non-Crystalline Solids, 172 (1994) 1001-1011.
[30] D.R. Day, T.J. Lewis, H.L. Lee, S.D. Senturia, The Role of Boundary Layer Capacitance at Blocking Electrodes in the Interpretation of Dielectric Cure Data in Adhesives, The Journal of Adhesion, 18 (1985) 73-90.
[31] S. Paszkiewicz, A. Szymczyk, I. Kasprowiak, M. Zenker, R. Pilawka, A. Linares, T.A. Ezquerra, Z. Rosłaniec, Electrical and rheological characterization of poly(trimethylene terephthalate) hybrid nanocomposites filled with COOH functionalized MWCNT and graphene nanosheets, Polymer Composites, 39 (2018) 2961-2968.
[32] D. Carponcin, E. Dantras, J. Dandurand, G. Aridon, F. Levallois, L. Cadiergues, C. Lacabanne, Discontinuity of physical properties of carbon nanotube/polymer composites at the percolation threshold, Journal of Non-Crystalline Solids, 392-393 (2014) 19-25.
[33] V. Trappe, W. Burchard, B. Steinmann, Anhydride-cured epoxies via chain reaction. 1. The phenyl glycidyl ether/phthalic acid anhydride system, Macromolecules, 24 (1991) 4738-4744.
[34] G.C. Stevens, Cure kinetics of a low epoxide/hydroxyl group-ratio bisphenol a epoxy resin–anhydride system by infrared absorption spectroscopy, Journal of Applied Polymer Science, 26 (1981) 4259-4278.
[35] M.C. Celina, N.H. Giron, M.R. Rojo, An overview of high temperature micro-ATR IR spectroscopy to monitor polymer reactions, Polymer, 53 (2012) 4461-4471.
[36] G. Nikolic, S. Zlatkovic, M. Cakic, S. Cakic, C. Lacnjevac, Z. Rajic, Fast fourier transform IR characterization of epoxy GY systems crosslinked with aliphatic and cycloaliphatic EH polyamine adducts, Sensors, 10 (2010) 684-696.